Nano Hybrids *Online: 2012-05-14*
ISSN: 2234-9871, Vol. 1, pp 1-22
doi:10.4028/www.scientific.net/NH.1.1

3-Mercaptopropionic acid capped Ga_2Se_3nanocrystal-CYP3A4 biosensor for the determination of 17-alpha-ethinyl estradiol in water

E. Nxusani, P.M. Ndangili, R.A. Olowu, A. N. Jijana, T. Waryo, N. Jahed,

R.F. Ajayi, P. Baker and E. Iwuoha*

Sensor Lab Department of Chemistry, University of the Western Cape, Bellville, 7535, South Africa

e-mail: 2861275@uwc.ac.za, pndangili@uwc.ac.za, rolowu@uwc.ac.za, 2505749@uwc.ac.za, twaryo@uwc.ac.za, njahed@uwc.ac.za, rngece@uwc.ac.za, pbaker@uwc.ac.za, *eiwuoha@uwc.ac.za (*Corresponding Author)

Keywords: endocrine disrupting compounds, nanocrystals, semiconductor, enzyme, electrochemical biosensor.

Abstract. Water soluble and biocompatible 3-mercaptopropionic acid capped gallium selenide nanocrystals, were synthesized from hydrated gallium (III) perchlorate and selenide ions. The 3-mercaptopropionic acid capped gallium selenide nanocrystals, was non-fluorescent but showed a sharp UV-vis absorption maximum at 250 nm.The synthesized nanoparticle was used to develop an electrochemical biosensor for the detection of 17-alpha-ethinyl estradiol, an estrogenic endocrine disrupting compound (e-EDC). The biosensor was fabricated by potentiostatic deposition of novel gallium selenide nanocrystals on a L-cystine modified gold electrode, followed by covalent coupling of genetically engineered cytochrome P450-3A4 (CYP3A4), a Heme containing enzyme. The biosensor gave an electrochemical response at about -220 mV. The results revealed that 3-Mecarptopropanoic acid capped Gallium Selenide nanocrystals can be used in conjunction with CYP3A4 as an electrode modifier for the detection of 17-alpha ethinyl estradiol. The 3-Mecarptopropanoic acid capped Gallium Selenide nanoparticles exhibited a semiconductor like behaviour.

Introduction

17-alpha-ethinyl estradiol (17EE), a natural/ synthetic hormone that is one of the main active elements in birth control pills and hormone replacement therapy, has been classified as an estrogenic endocrine compound (e-EDC). Naturally occurring hormones, such as 17EE, are involved in the control of the early mitotic proliferation phase of germ cells during spermatogenesis in males [1-2] and takes part in regulation of final oocyte maturation and ovulation in females [3-42]. Due to the ability of 17EE to alter the sexual behavior of animals and because of their ubiquitous nature, the need for detection of trace amounts of this chemical using simple, low cost, highly sensitive, low detection range, highly selective and easy to handle techniques becomes necessary.

Conventional methods have been reported for the detection of estrogenic endocrine disruptors. These include methods such as chemiluminescence enzyme immunoassay [5,6], high performance liquid chromatography (HPLC) [7,8,9], as well as enzyme linked Immunosorbent assay (ELISA) [10]. But since they are expensive, and require complex pre-treatment, long analysis time and compound recovery systems, scientists have placed their focus on alternatives such as biosensors. Biosensors are electrochemical transducers that employ a bio-recognition element as the basis of their detection. Several biosensors have been developed for the quantification of endocrine disruptors such as 17β-estradiol [11, 12, 13] using different electrode modification techniques.

Cytochrome P450 iso-enzyme, CYP3A4, is the most catalytically versatile, having the ability to catalyze the oxidative metabolism of various xenobiotic compounds which includes chlorophenols, pesticides, carcinogens, etc [14,15,16,17]. In this transducer, CYP3A4 oxidatively metabolizes 17EE to estrone as described in (Fig.1). Though this cycle involves electronic transfer but this is very poor for electrochemical detection, thus we have employed nanoparticles as part of our electrode modification.

Metal selenide semiconductor nanocrystals, or nanoparticles are receiving remarkable research attention because of their size-dependent optical and electrical properties [18]. Among the many metal selenide known, gallium selenide which is a member of III–VI group has a number of interesting properties for electrical and nonlinear optical applications [19,20]. In fact, thin films of III–VI group materials are potential alternatives to II–VI group materials in optoelectronic and photovoltaic devices and also have a potential application as passivating layers for III–V devices [21,22]. When functionalized with amphiphilic bi-functional molecules such as mercapto carboxylic acids [HS- (CH2)n-COOH, n = 1–15] [24], the small sizes of nanoparticles can enhance the transfer of electrons during analysis [25]. The small sizes of the nanoparticles increase the surface area of the electrode thus affording more binding sites for the enzyme. A high amount of enzyme on the electrode surface increases the rate of diffusion of the analyte towards the electrode [11]. Also, the carboxylic group offers a biocompatible surface since it can react favourably with the amino group of enzyme without loss of enzyme activity. Short chained capping agents such as mercaptopropionic acid (MPA) have been used for self-assembly on gold electrode [26] and are associated with enhanced electrochemical signals of the quantum dots towards target analytes [27]. This paper describes an approach for the determination of 17EE using 3-mercaptopropionic acid capped Ga_2Se_3 nanoparticles/ CYP3A4 modified gold electrode.

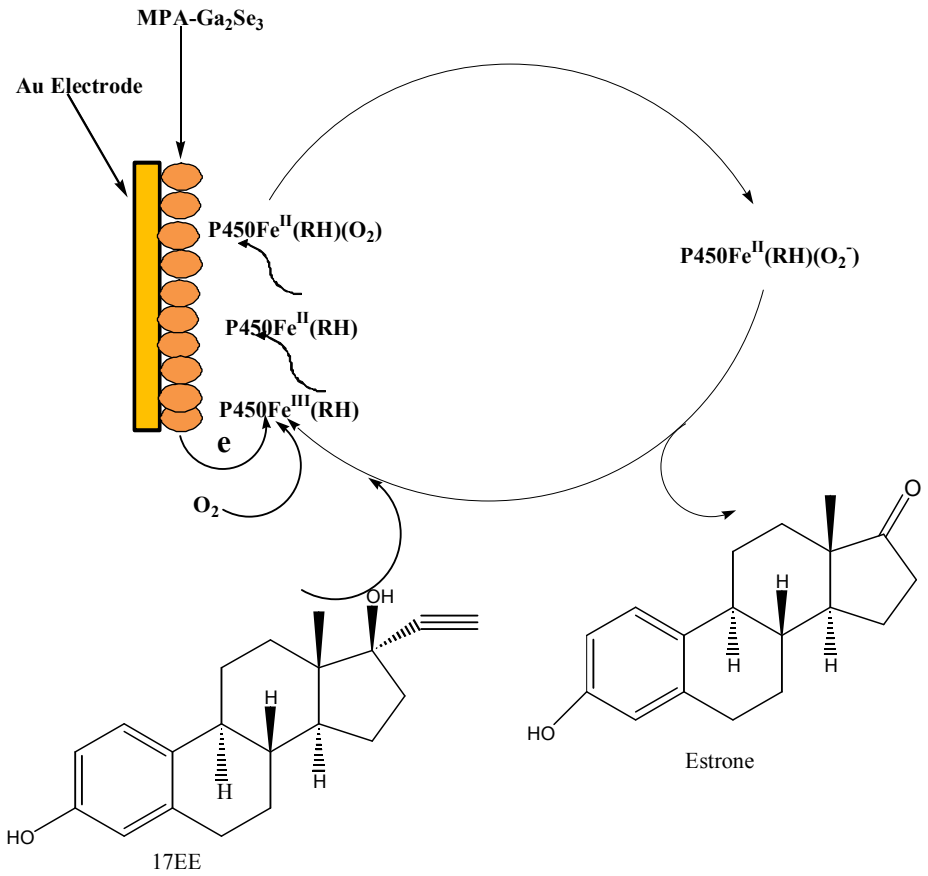

Fig. 1. Metabolism of 17EE by CYP3A4 to estrone

Experimental section

Chemicals and Reagents. Analytical grade zinc nitrate hexahydrate, 3-mercaptopropionic acid ($HSCH_2CH_2CO_2H$) [3-MPA], sodium hydroxide, selenium powder, sodium borohydrate, gallium, perchloric acid disodium hydrogen phosphate, sodium dihydrogen phosphate, potassium ferricyanide, potassium ferrocyanide, 1-ethyl-3-(3-dimethylaminopropyl) carbodiimide hydrochloride (EDC) and N-hydroxysuccinimide (NHS), L-cystine, ethanol, 17-alpha ethinyl-estradiol, ethanol were of analytical grade and were all purchased from Sigma-Aldrich (Cape Town, South Africa). 0.10 M phosphate buffer solution, pH 7.40, was prepared from disodium hydrogen phosphate and sodium dihydrogen phosphate. 5 mM (1:1) solution of $K_3Fe(CN)_6$ and $K_4Fe(CN)_6$ was prepared in 100 mL of PBS at pH 7.5

Genetically engineered cytochrome P450-3A4 (CYP3A4), purified from a full length human CYP3A4 DNA clone, with a stock concentration of 37.74 μM was purchased from Merck South Africa while Alumina micro polish and polishing pads were obtained from Buehler, IL, USA and were used for polishing the gold electrode before any modification.

Electrochemical measurement. A 10 mL electrochemical cell with a conventional three electrode set up was used to perform all electrochemical experiments. A gold electrode from BAS with an area of 0.0201 cm^2 was used as the working electrode, platinum wire from Sigma Aldrich as the counter electrode, and Ag/AgCl (3 M Cl^-) as the reference electrode. All voltammetric measurement were carried with BAS100W integrated and automated electrochemical work station from Bio Analytical Systems (BAS), Lafayette, USA. All voltammograms; both cyclic and square wave, were recorded with a computer interfaced to the BAS 100W electrochemical workstation. Electrochemical impedance spectroscopy (EIS) measurements were recorded with Zahnner IM6 electrochemical workstation (MeBtechnik).

Ultra violet-visible (UV-vis) absorption measurements were made on a Nicolet Evolution 100 UV–visible spectrometer (Thermo Electron, UK), using a quartz cuvette. AFM was done with Nanosurf easy scan AFM system version 2.2.

Methodology

Synthesis of 3-mercaptopropionic acid capped Ga_2Se_3 nanocrystals. 4.87 g of Ga metal was weighed into a round bottomed flask and 2 mL of concentrated $HClO_4$ added. The mixture was refluxed under constant stirring for 4 h at 120 °C, after which, a white precipitate of $Ga(ClO_4)_3.6H_2O$ was formed. 0.19 g of the gallium salt was dissolved in 10 mL of distilled water and 69.60 μL of concentrated MPA added. The pH of the solution was adjusted to 12 using NaOH and saturated with N_2 for 30 min. Then the Se^{2-} was prepared by mixing 0.016 g of Se powder with 0.015 g of NaBH4 in a round bottomed flask and adding de-ionized water to make 10 mL solution, which resulted to 0.02 M and 0.04 M of Se and NaBH4, respectively. The mixture was then stirred

continuously at room temperature under nitrogen saturation for 25 min after which a dark yellow solution was formed. Freshly prepared Se^{2-} was then added drop wise into the nitrogen saturated $Ga(ClO_4)_3$/3MPA solution. After 10 min, a brown solution was formed and the reaction was quenched by immediately placing the reaction flask in a freezer at -20 °C.

Construction of the CYP3A4 biosensor. A new Au electrode was polished with 1, 0.5 and 0.03 μm alumina slurries on separate glassy polishing pads respectively. After polishing, the electrode was ultrasonicated for about 15 min, with distilled water and absolute ethanol to remove any possible absorbed alumina crystals on the electrode surface and rinsed carefully with distilled water. The clean Au electrode was then immersed into a solution containing 0.02 M L-cystine solution at room temperature for 24 h in the dark, to form self-assembled monolayer onto the gold electrode. The electrode was then rinsed carefully with distilled water to remove any unbound L-cystine molecules. The cysteine modified electrode was then activated by dipping into a solution containing 1:1 of EDC and NHS, for 20 min which was followed by immersion into the gallium selenide nanocrystals functionalized with mercaptopropionic acid (MPA) solution, for 2 h to form Ga_2Se_3/L-cystine modified gold electrode. The resulting quantum dot modified gold electrode was allowed to dry for some time under nitrogen gas. 3 μL of a 4 μM CYP3A4 enzyme solution was then drop coated onto the Ga_2Se_3 modified electrode surface and allowed to dry for 3 h at 2 °C. This process of modification resulted into fabrication of CYP3A4/ Ga_2Se_3 /L-cystine/Au biosensor. The biosensor was then stored at 2 °C in 0.1 M PBS of pH 7.4 when not in use.

Biosensor measurements. All the electrochemical measurements were carried out in 0.1 M PBS as the supporting electrolyte at room temperature, 25 °C. An analyte solution of 0.031 mM 17-alpha ethinyl estradiol was prepared using 0.1 M PBS solution. The substrate measurements were carried out under anaerobic conditions.

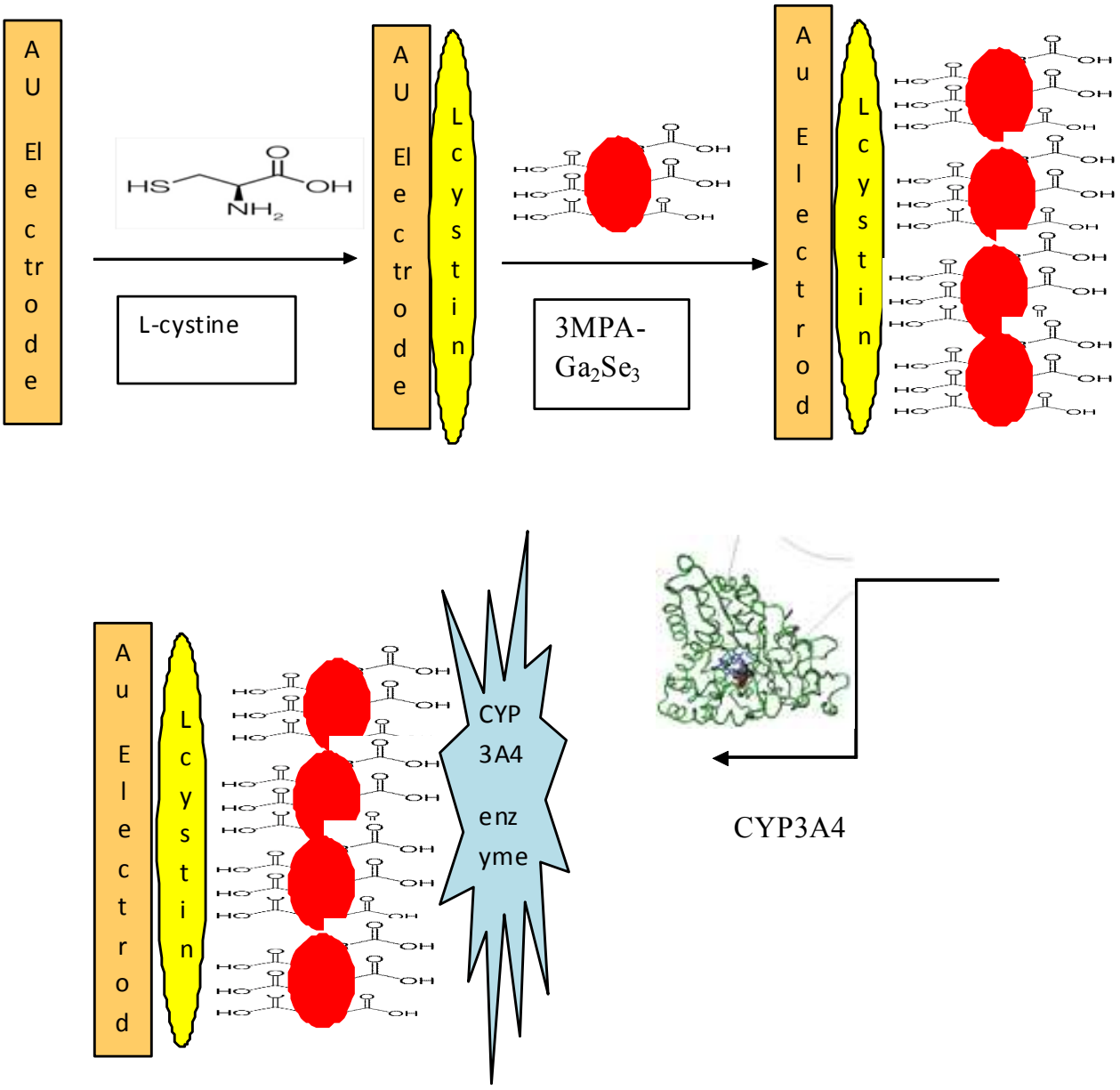

Fig. 2. Schematics for the development of the CYP3A4/Ga_2Se_3/L-cystine/Au biosensor

Results and Discussion

Spectroscopy of the 3MPA-Ga_2Se_3 nanocrystals. The UV-vis absorption spectrum of the Ga_2Se_3-3MPA in Figure. 3 shows a broad absorption maximum at 250 nm. This is an indication that the particle size distribution is inhomogeneous which may be attributed to the interferences from the sample matrix, such as the capping agent of the nanocrystals (3-mercaptopropionic acid) and the $NaBH_4$ which was used during synthesis.

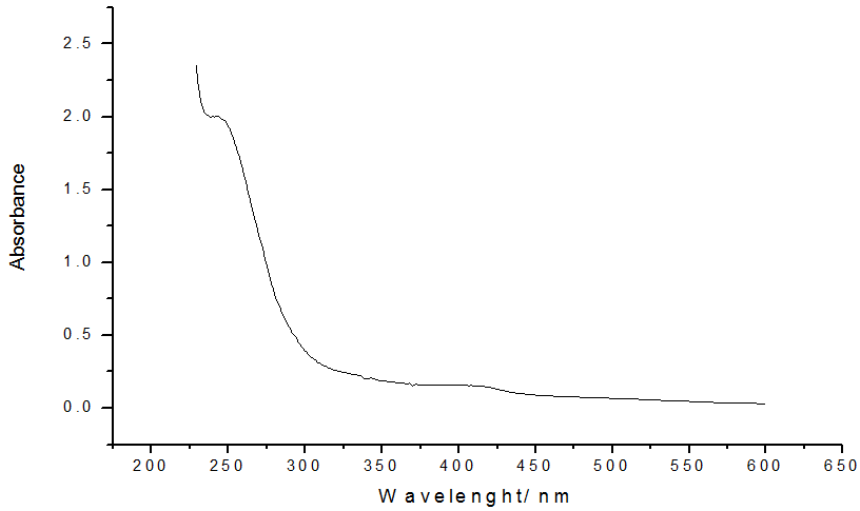

Fig. 3. UV-vis spectrum of 3MPA-Ga_2Se_3 nanoparticles.

Usually, the nature of the interaction between the conduction and valence bands as well as the size of the band gap determines the optical properties of semiconducting nanocrystals. The absorption of a photon by a Ga_2Se_3 nanocrystal causes electronic transition from the valence band to the conduction band, which creates an electron-hole pair known as an exciton in the valence band. The lowest-energy electron-hole pair (excitonic) state ($1S_{3/2}$-$1S_e$) is not usually observable in nanocrystals that are heterogeneous in size, shape and composition. However, more homogeneous nanocrystals exhibit more sharp absorption peaks.

Electrochemical interrogation of the 3MPA-Ga2Se3 nanocrystals

Electrochemical impedance Spectroscopy (EIS) of Au/3MPA-Ga2Se3. EIS measurements were performed in the presence of 5 mM $[K_3Fe(CN)_6]$/[$K_4Fe(CN)_6$] at a potential of 220 mV and at a frequency range of 0.1 to 10^5 Hz; the amplitude of the alternate voltage was 10 mV. R_{ct} represents the resistance to the charge transfer between the electrolyte and the electrode and this gives information on the electron transfer kinetics of the redox probe at the electrode interface. The modification of the electrode with the nanocrystals changes the capacitance and the interfacial electron transfer resistance of the electrode. In the Nyquist diagram the semicircle observed at

higher frequency, corresponds to the electron limited process whereas the linear part is the characteristics of the lower frequency range and represents the diffusion limited electron transfer process. The impedance response of the bare and Au modified electrode are depicted in Figure 4, with bare Au and Au/3MPA-Ga_2Se_3 electrodes having an R_{ct} values of 104.4 and 2313.48 Ω, respectively.

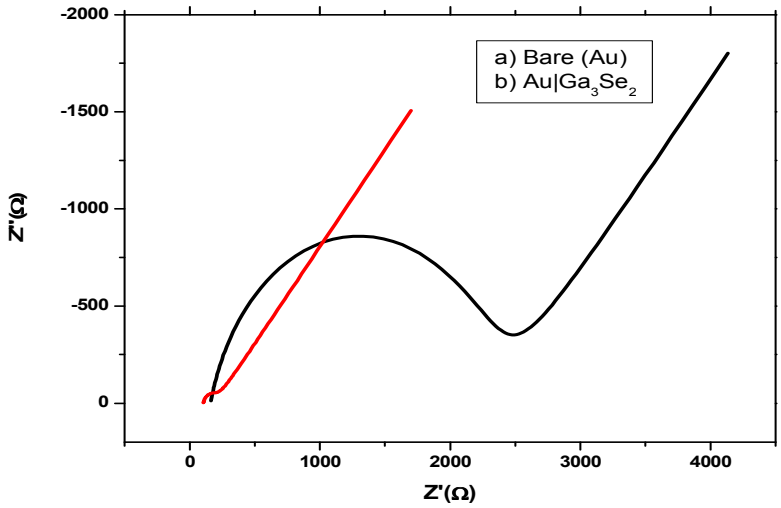

Fig. 4. Nyquist plots of bare Au and Au/Ga_2Se_3-3MPA in 5.00 mM $[Fe(CN)_6]^{-3/-4}$

The bare Au electrode exhibited a very small semi circle at lower frequency. After the assembly of the 3MPA-Ga_2Se_3 nanocrystals on the Au electrode, the R_{ct} value increased 10 fold. The increase was found to be 95.5 % in comparison to the bare. This is attributed to the presence of the 3MPA-Ga_2Se_3 nanocrystals, which played a major role in decelerating the charge transfer of the electrons. The deceleration is highly due to the electrostatic repulsion between the Ga_2Se_3-3MPA nanocrystals and $[Fe(CN)_6]^{3-/4-}$ redox probe which are both negatively charged. This behavior is intrinsic to semiconducting materials.

Kinetic parameters such as exchange current (i_0) , time constant and rate constant was calculated to substantiate rate of electron transfer behaviour of the bare electrode and the Ga_2Se_3-3MPA nanocrystals modified Au electrode. The i_0 of the system is given by:

$$i_0 = RT/nFR_{ct} \quad [1]$$

where n is the number of electrons transferred, F is the Faraday constant (96,584 C mol^{-1}), R is the gas constant (8.314 J mol^{-1} K^{-1}), T is the reaction temperature (298 K). The i_0 value for the electron transferred reaction of the redox probe ($[Fe(CN)_6]^{3-/4-}$) on the bare and Au|3MPA-Ga_2Se_3 were 2.46 $\times$ 10^{-4} A and 1.11 $\times$ 10^{-5} A, respectively. From the calculated value it can be deduced that the rate of electron transfer was faster on the bare Au electrode than on the Au/3MPA-Ga_2Se_3 platform.

Heterogeneous rate constant of the system is given by:

$$i_0 = nFAk^0C^* \quad [2]$$

where i_0 is the exchange current (A), A is the geometric area of the electrode (0.021 cm^2), k^0 is the heterogeneous rate transfer constant (cm s^{-1}) and C^* is bulk concentration of $[Fe(CN)_6]^{3-/}4$. The k^0 values for the bare and Au/3MPA-Ga_2Se_3 were 2.42 $\times$ 10^{-5} cm s^{-1} and 1.10 $\times$ 10^{-6} cm s^{-1}. The larger value of k^0 for Au electrode supports the theory that the semi-conducting 3MPA-Ga_2Se_3 impeded the charge transfer of the $[Fe(CN)_6]^{3-/4-}$ redox probe.

The time constant value for the bare Au and Au/3MPA-Ga_2Se_3 electrode are 1.11 $\times$ 10^{-4} s/rad and 8.74 $\times$ 10^{-4} s/rad, respectively; and it showed that the Faradaic process of the $[Fe(CN)_6]^{3-/4-}$ probe is slower on the Au/3MPA-Ga_2Se_3 electrode than on the bare electrode. These results complemented the UV-vis results displayed in Fig. 3. The Nyquist plot for the nanocomposite showed a large semi circle, which is characteristic to an electron limited process.

Cyclic voltammetry (CV) response of Au/3MPA-Ga_2Se_3. Cyclic voltammetry (CV) is considered to be the most versatile electro-analytical technique currently available. Cyclic voltammetry of the Au/3MPA-Ga_2Se_3 in 5.00 mM $[Fe(CN)_6]^{-3/-4}$ (Fig. 5) showed a wider redox peak separation (ΔE_p) than for Au; and a 50 % decrease in peak currents. The cyclic voltammetric

behaviour of the modified electrode indicates a more sluggish electron transfer rate at the 3MPA-Ga_2Se_3/$[Fe(CN)_6]^{-3/-4}$ interface compared to Au/$[Fe(CN)_6]^{-3/-4}$and corroborates the electrostatic repulsion phenomenon observed in EIS.

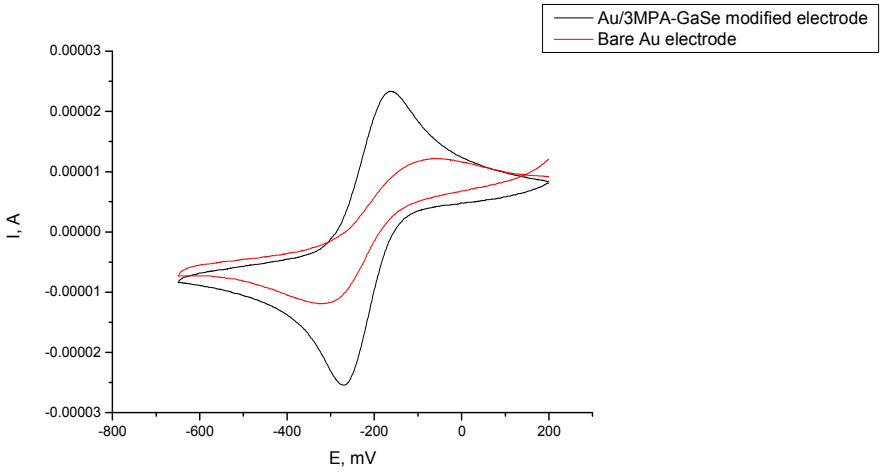

Fig. 5. Cyclic voltammograms of bare Au and Au/3MPA-Ga_2Se_3 in 5.00 mM $[Fe(CN)_6]^{-3/-4}$ at 100 mV/s.

Electrochemical characterization of the Biosensor modification. Fig. 6 and 7 showed the cyclic voltammograms of the L-cystine and the 3MPA-Ga_2Se_3 nanocrystal modified electrodes respectively. It is noted that upon the immobilization of the L-cystine there appears a reduction peak and an oxidation around 200 mV. Further modification of electrode with the 3MPA-Ga_2Se_3 nanocrystals caused the disappearance of these peaks which indicate that the nanocrystals were successfully immobilized on the electrode surface.

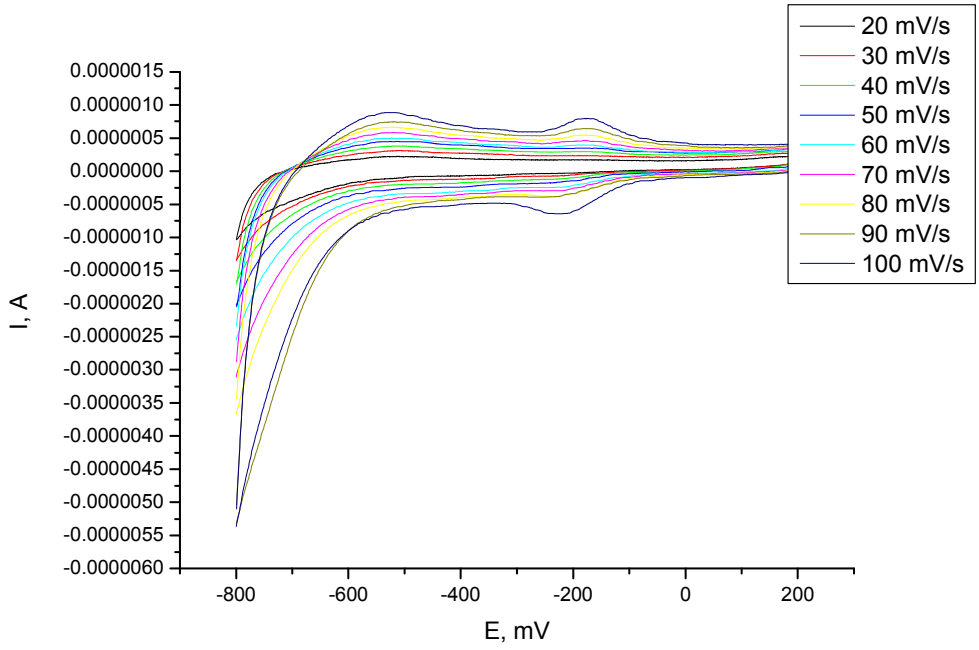

Fig. 6. Cyclic voltammogram of Au/L-cystine modified electrode in 0.10 M phosphate buffer pH 7.4 at different scan rates.

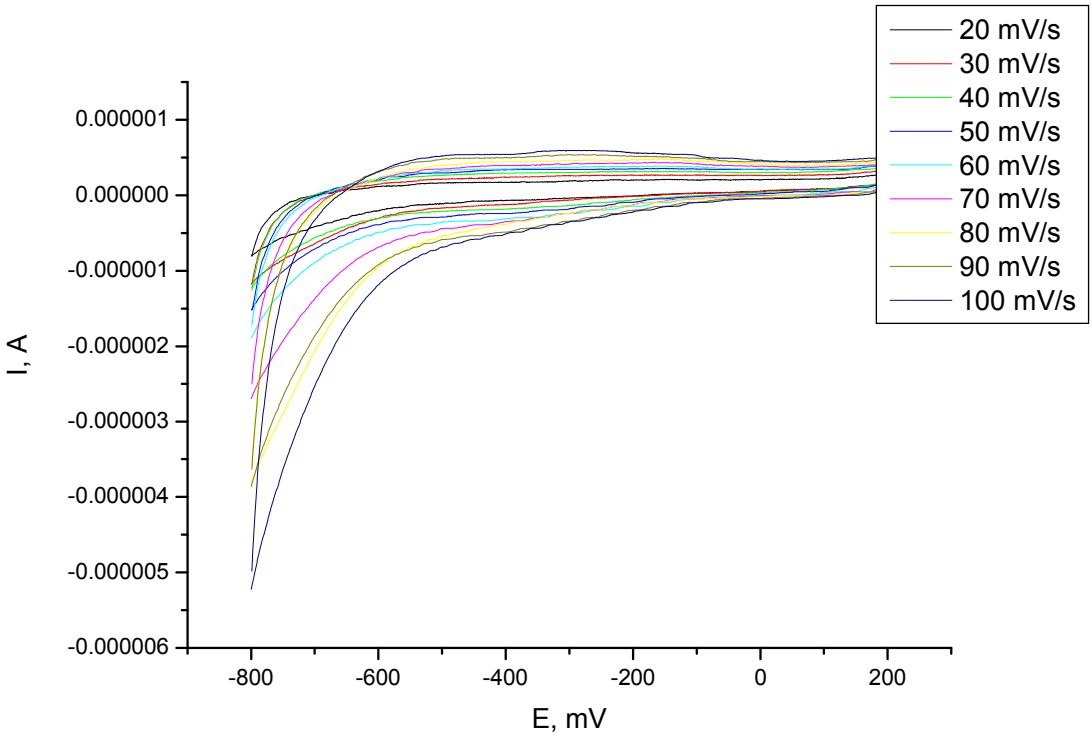

Fig. 7. Cyclic voltammogram of Au/Cystine/3MPA-Ga_2Se_3 modified electrode in 0.10 M phosphate buffer pH 7.4 at different scan rates.

Atomic Force Microscopy (AFM). The Atomic Force Microscope (AFM) is a tool currently being used to solve processing and material problems in a wide range of technologies affecting the electronics, telecommunications, biological, chemical, automotive, aerospace, and energy industries. The materials being investigated include thin and thick film coatings, ceramics, composites, glasses, synthetic and biological membranes, metals, polymers, and semiconductors. The AFM is applied to studies of phenomena such as abrasion, adhesion, cleaning, corrosion, etching, friction, lubrication, plating, and polishing. Figure 8, showed the AFM study of the surface roughness of the gold electrode upon each step of modification.

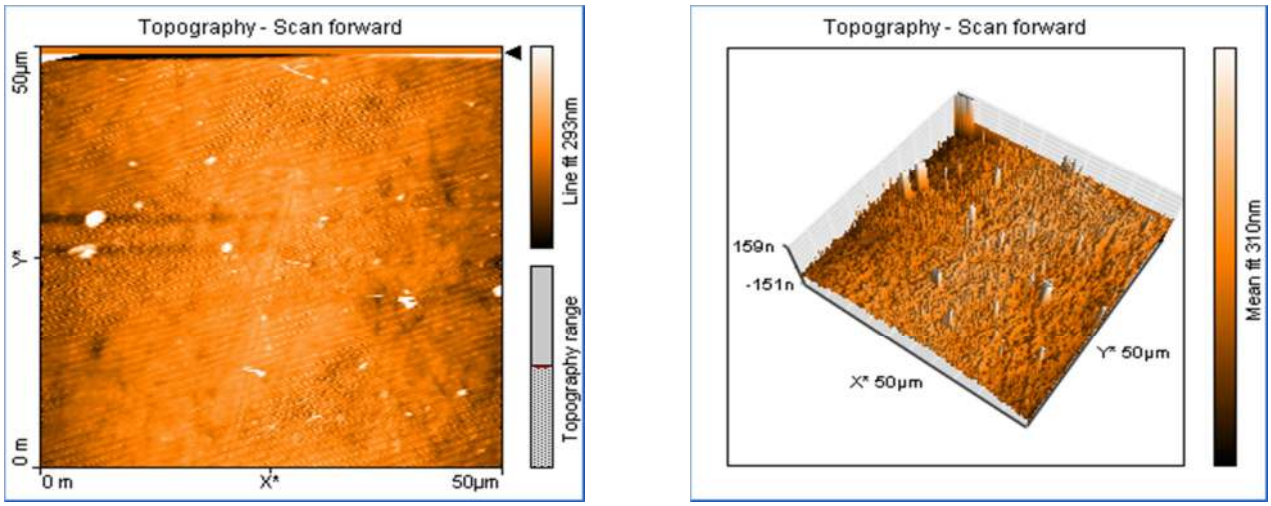

(a)

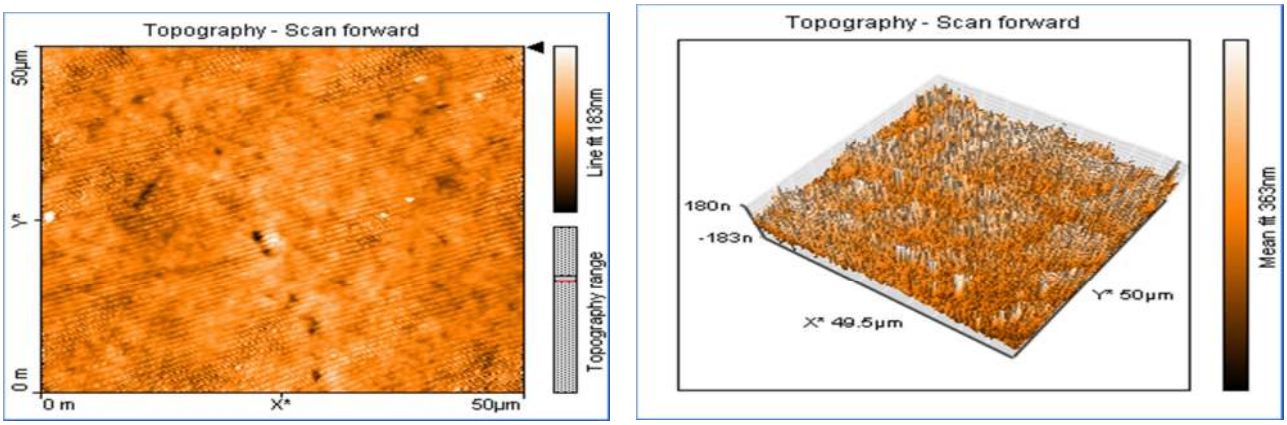

(b)

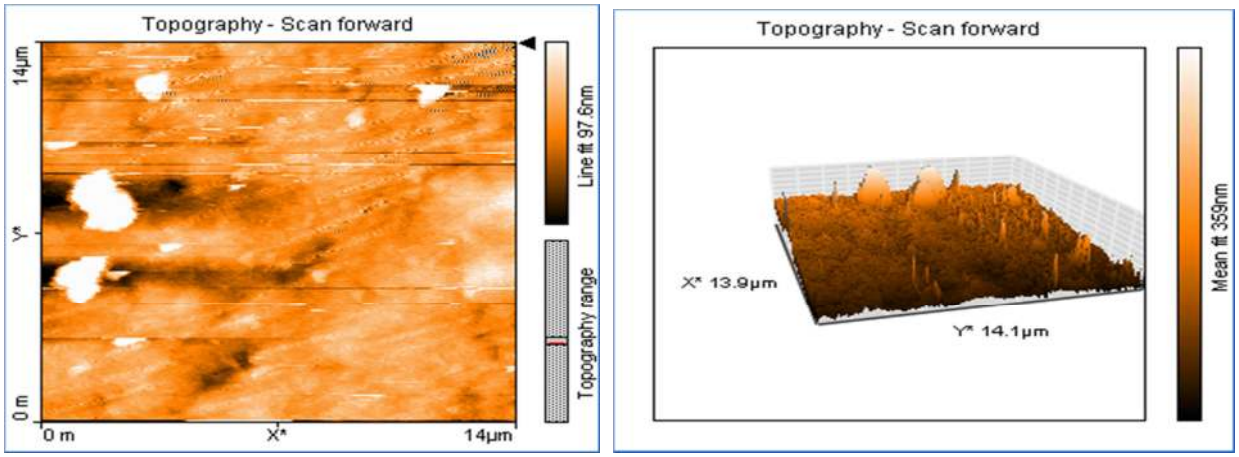

(c)

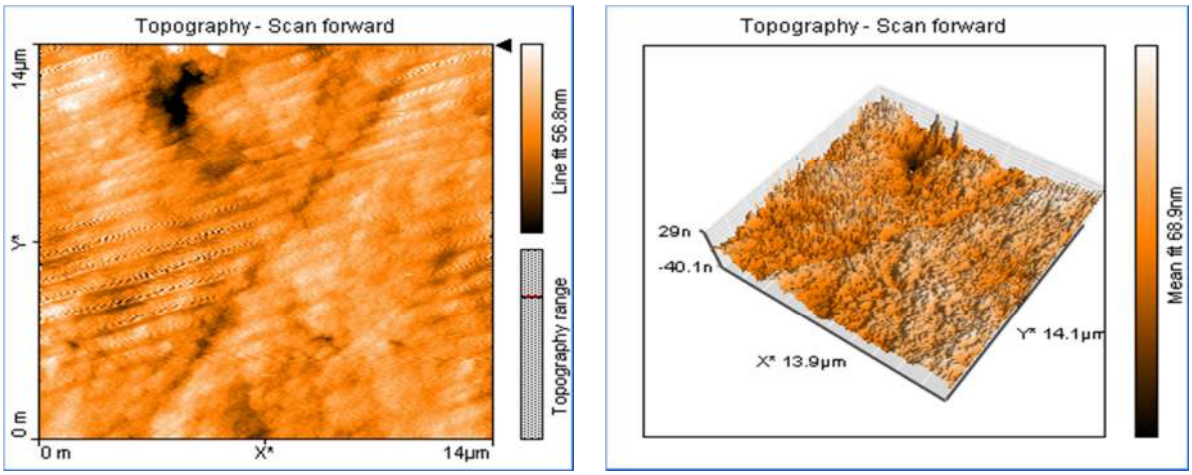

(d)

Fig. 8. AFM micrographs of (a) Bare Au, (b) Au/L-cystine, (c)Au/L-cys/3MPA-Ga_2Se_3, (d) Au/L-cys/3MPA-Ga_2Se_3/CYP3A4 modified electrode.

The results are summarized in the following graph:

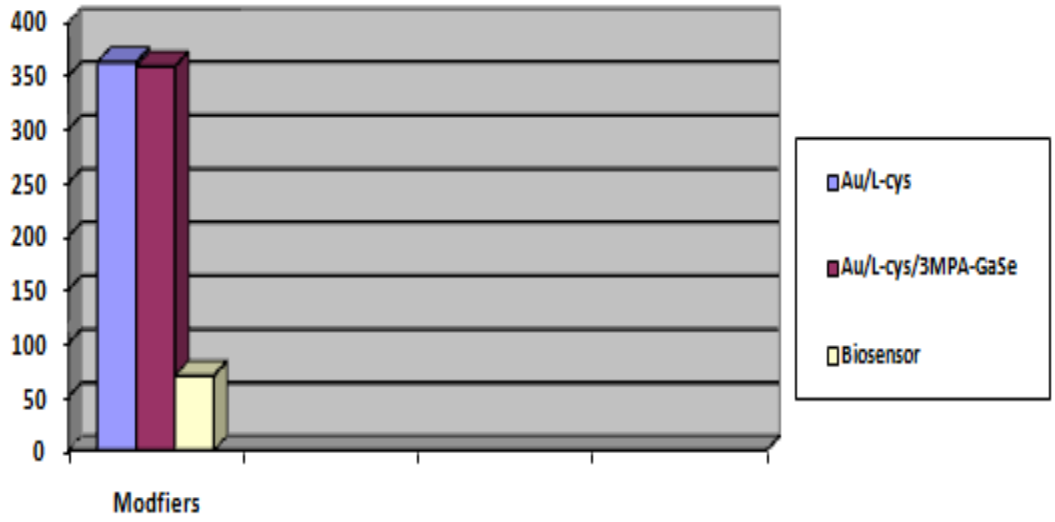

Fig. 9. Representation of the surface roughness of Au/L-cystine modified electrode, Au/L-cys/3MPA-Ga_2Se_3 modified electrode and Biosensor.

The AFM micrographs showed that the surface of the Au/L-cystine electrode exhibited a high surface roughness compared to the when the electrode was modified with CYP3A4 to form a biosensor which showed smoother surface. This can be explained by the fact that upon, the immobilization of the CYP3A4, most of the reaction sites are then occupied through the covalent bonding of the amine groups of the enzyme and the carboxylic groups of the 3-mercaptoproponic acid, thus giving rise to a uniform coverage and further giving assertion that the biosensor construction was successful.

Biosensor Response to successive additions of 17-alpha ethinyl estradiol (17EE) in phosphate buffer of pH 7.4 at 40 mV/s. Cyclic voltammetry (CV) and square wave voltammetry (SWV) were used to study the catalytic activity of the Au/L-cys/3MPA-Ga_2Se_3/CYP3A4 biosensor. All the Voltammetric measurements were carried out under aerobic conditions at room temperature. The oxygen was necessary for the CYP3A4 active site, Fe^{3+}, which binds with oxygen to form Fe-O

redox centre. The oxygenated iron centre of the CYP3A4 is known to be more active than unoxygenated Fe^{3+} centre, thus allowed for a rapid substrate reduction, and fast enzyme- substrate kinetics.

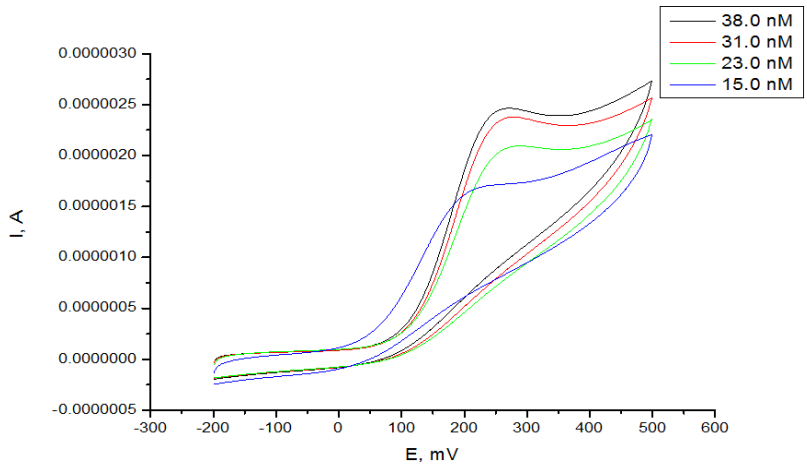

Fig. 10. Cyclic voltammograms of Au/L-cys/3MPA-GaSe/CYP3A4 biosnsor response to successive additions of 17EE in phosphate buffer of pH7.4 at 40 mV/s

The response of the biosensor to 17-alpha ethinyl estradiol substrate was studied at a potential window of -500 mV to 200 mV were the characteristic reduction peak of the enzyme usually appears as reported in many CYP3A4 assays.

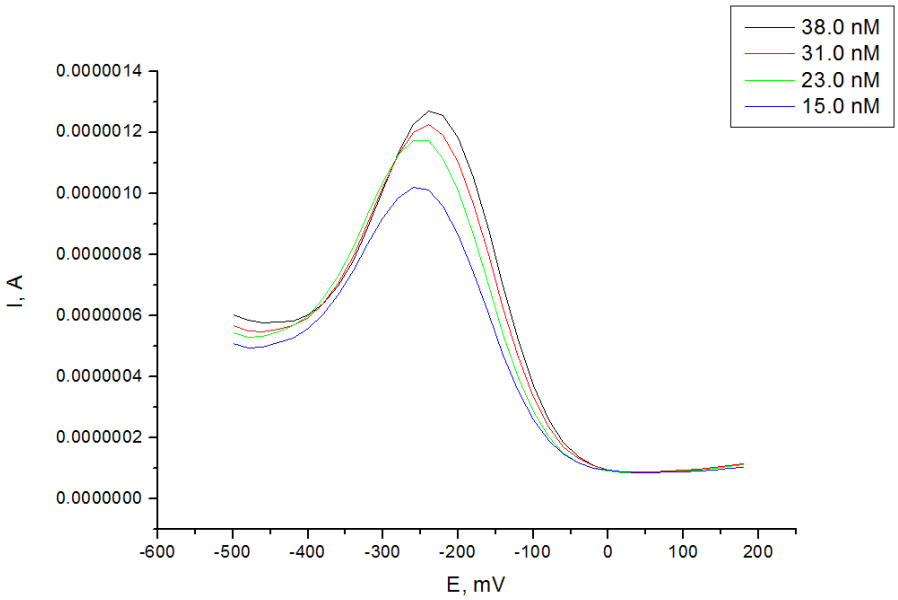

Fig. 11. Square wave voltammograms of Au/L-cystine/3MPA-GaSe/ CYP3A4 biosensor response to successive additions of 17EE in phosphate buffer at 40 mV/s.

Upon successive additions of 17EE into the 0.1 M PBS (Fig.10), there was an appearance of reduction peak that occurred at a potential of -220 mV, the peak was an indication that the presence of 17EE induced an increase in the rate of dioxygen binding to the heme group of the CYP3A4. The catalytic reduction of 17-alpha ethinyl estradiol was then found to be irreversible, due to the absence of oxidation peak couple.

In Fig. 11, the square wave voltammetric (SWV) response of the biosensor at different concentrations of 17 alpha-ethinyl estradiol is shown. The biosensor gave a similar response of SWV as that of the cyclic voltammetry. In the factor of increasing the concentration of 17 alpha-ethinyl estradiol, there was an increase in the reduction peak current at a potential of E_p = -220 mV. The SWV reduction peaks gave an amplification of the observed peaks of the CV.

Controlled Experiments. A set of controlled experiments was performed to evaluate the response of the biosensor. This was done to pin-point the exact modifier which is responsible for the biosensor response in detecting 17-alpha-ethinyl estradiol. As shown in Figure 12, upon addition of 54.25 nM 17-alpha-ethinyl estradiol on the bare electrode, there was no response at all as expected. On the Au/L-cystine modified electrode no reduction peak was observed, thus also no notable response. The Au/L-cys/3MPA-Ga_2Se_3 modified electrode showed a very slight response and on the biosensor, a very distinct response was observed. This means that the response of the biosensor is due to the 3MPA-Ga_2Se_3 and the enzyme, as it has been expected.

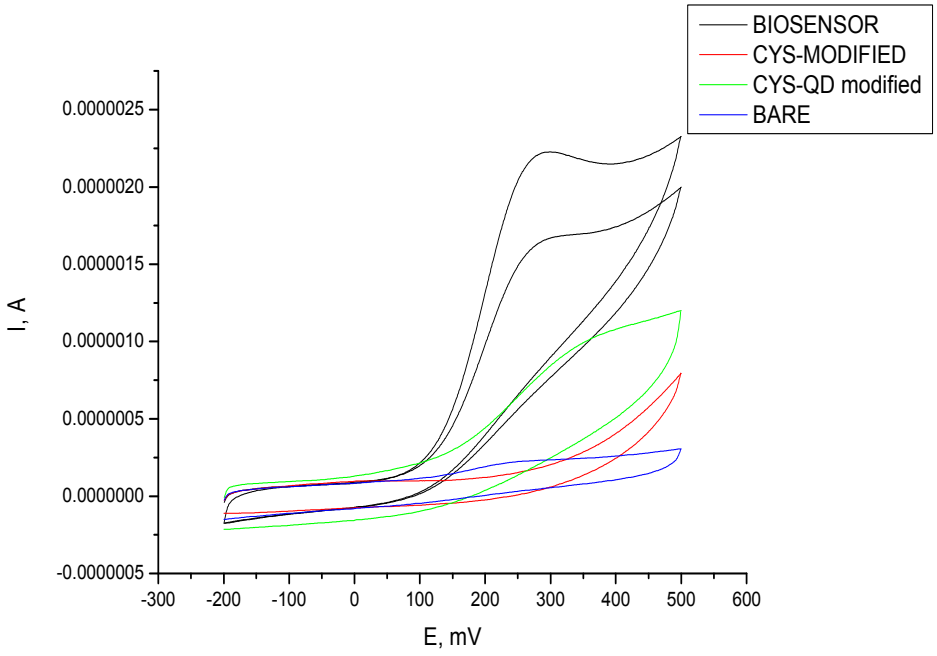

Fig. 12. Cyclic Voltammograms showing response of each layer of the electrode modifiers in the presences of 54.25 nM 17-alpha ethinyl estradiol in pH 7.4 buffer solution.

Conclusion

The nanobiosensors produced with 3-mecarptopropanoic acid-capped gallium selenide nanoparticles and CYP3A4 is characterised by very low detection potential of -220 mV. This makes it an appropriate for the fabrication of energy serving and battery-operated sensor devices for field application. The sensor exhibits very low detection limits for 17-alpha-ethinyl estradiol in aqueous medium. The quantum dot biosensors device is therefore very suitable for application in the determination of very low levels of 17EE in both municipal wastewater and in drinking water.

Acknowledgements

Miss E. Nxusani is grateful to research Centre for Scientific and Industrial Research (CSIR), South Africa for the award of scholarship. We are grateful to the Water Research Commission (WRC) of South Africa for award of the ENDOTEK research grant that funded this study.

References

[1] B. Campbell, J.T. Dickey, and P. Swanson, Endocrine Changes During Onset of Puberty in Male Spring Chinook Salmon, Oncorhynchus tshawytscha. Biology of Reproduction, 69(6) (2003) 2109-2117.

[2] T. Miura, and C.I. Miura, Molecular control mechanisms of fish spermatogenesis. Fish Physiology and Biochemistry, 28(1) (2003) 181-186.

[3] R.E. Peter. and K.L. Yu, Neuroendocrine regulation of ovulation in fishes: basic and applied aspects Reviews in Fish Biology and Fisheries, 7 (1997) 173-197.

[4] D.E. Kime, ‘Classical' and 'non-classical' reproductive steroids in fish. Reviews in Fish Biology and Fisheries 3 (1993) 160-180.

[5] L. Zhao, Z. Li, X. Ying, J. M. Lin, Development of a highly sensitive, second antibody format chemiluminescence enzyme immunoassay for the determination of 17β-estradiol in wastewater. Anal.Chim. Acta, 558(1-2) (2006) 290-295.

[6] H. B. Wei, J. M. Lin, D. N. Wu, L.X. Zhao, Z .J. Li, Detection of 17β-Estradiol in River Water and Human Urine by Highly Sensitive Chemiluminescence Enzyme Immunoassay. Chinese J Anal. Chem. **35**(3) (2007) 319-324.

[7] J.A. Russell, R. K. Malcolm, K. Campbell, High-performance liquid chromatographic determination of 17β-estradiol and 17β-estradiol-3-acetate solubilities and diffusion coefficients in silicone elastomeric intravaginal rings. J Chromatog. B: Biomed. Sci. and Appl.744(1) (2000) 157-163.

[8] Y. Yoon, P. Westerhoff, S.A. Snyder, HPLC-fluorescence detection and adsorption of bisphenol A, 17β-estradiol, and 17α-ethynyl estradiol on powdered activated carbon. Water Research,. 37(14) (2003) 3530-3537.

[9] A. Mishra and K.P. Joy, HPLC-electrochemical detection of ovarian estradiol-17β and catecholestrogens in the catfish Heteropneustes fossilis: Seasonal and periovulatory changes. General and Comparative Endocrinology, 145(1) (2006) 84-91.

[10] G. Volpe, G. Fares, F. delli Quadri, R. Draisci, G. Ferretti, C. Marchiafava, D. Moscone, and G. Palleschi, A disposable immunosensor for detection of 17β-estradiol in non-extracted bovine serum. Anal. Chim. Acta, 572(1) (2006) 11-16.

[11] P. M. Ndangili, A. M. Jijana, P. G.L. Baker E. I. Iwuoha, 3-Mercaptopropionic acid capped ZnSe quantum dot-cytochrome P450 3A4 enzyme biotransducer for 17β-estradiol. J Electroanal. Chem.. 653(1-2) (2011) 67-74.

[12] Y. S. Kim, H. S. Jung, T. Matsuura, H. Y. Lee, T. Kawai, M. B. Gu,. Electrochemical Detection of 17β-estradiol Using DNA Aptamer Immobilized Gold Electrode Chip. Biosens. Bioelect. 22 (2007) 2525-2531.

[13] R. A. Olowu, O. Arotiba, S. N. Mailu, T. T. Waryo, P. Baker, and E. Iwuoha Electrochemical Aptasensor for Endocrine Disrupting 17β-Estradiol Based on a Poly (3,4-ethylenedioxylthiopene)-Gold Nanocomposite Platform. Sensors (10) **(**2010) 9872-9890.

[14] N. Bistolas, U. Wollenberger, C. Jung, Cytochrome P450 biosensors—a review. Biosen and Bioelect. 20(12) (2005) 2408-2423.

[15] A. P. Li, D. . Kaminski and A. Rasmussen, Substrates of human hepatic cytochrome P450 3A4. Toxicology, 104(1-3) (1995) 1-8.

[16] M. T. Donato and J. V. Castell, Strategies and Molecular Probes to Investigate the Role of Cytochrome P450 in Drug Metabolism: Focus On In Vitro Studies. Clinical Pharmacokinetics,. 42(2) (2003)153-178.

[17] V. V. Shumyantseva, T. V. Bulko and A. I. Archakov, Electrochemical reduction of cytochrome P450 as an approach to the construction of biosensors and bioreactors. J Inorg. Biochem. 99(5) (2005) 1051-1063.

[18] Z. A Peng and X. Peng, Mechanisms of the Shape Evolution of CdSe Nanocrystals. J Am Chem Soc, 123(7) (2001) 1389-1395.

[19] K. Ueno, S. Tokuchi, K. Saiki, Epitaxial growth of a vacancy-ordered Ga2Se3 thin film on a vicinal Si(001) substrate. J Crys. Growth, 237-239, Part 2 (2002) 1610-1614.

[20] C. E. M. Campos, J. C. de Lima, T. A. Grandi, K. D. Machado and P. S. Pizani, GaSe formation by mechanical alloying $Ga_{50}Se_{50}$ mixture. Solid State Commun, 126(11) (2003) 611-615.

[21] J-H. Park, M. Afzaal, M. Helliwell, M. A. Malik, P. O'Brien and J. Raftery, Chemical Vapor Deposition of Indium Selenide and Gallium Selenide Thin Films from Mixed Alkyl/Dialkylselenophosphorylamides. Chem. Mat., 15(22) (2003) 4205-4210.

[22] M. Lazell, P. O'Brien, D. J. Otway and J.-H. Park, Single source molecular precursors for the deposition of III/VI chalcogenide semiconductors by MOCVD and related techniques. J. Chem. Soc. Dalton Transactions, 24 (2000) 4479-4486.

[23] J. Aldana, Y. A. Wang and X. Peng, Photochemical Instability of CdSe Nanocrystals Coated by Hydrophilic Thiols. J Am Chem Soc. 123(36) (2001) 8844-8850.

[24] M. Liu, G. Shi, L. Zhang, Y. Cheng, L. Ji, Quantum dots modified electrode and its application in electroanalysis of hemoglobin. Electrochem Commun, 8(2) (2006) 305-310.

[25] M. J., Giz, B. Duong, and N. J. Tao, In situ STM study of self-assembled mercaptopropionic acid monolayers for electrochemical detection of dopamine. Journal of Electroanalytical Chemistry, 465(1) (1999) 72-79.

[26] J. Li, G. Zou, X. Hu and X. Zhang, Electrochemistry of thiol-capped CdTe quantum dots and its sensing application. J. Electroanal. Chem., 625(1) (2009) 88-91.